Guest water-induced structural transformation and spin-crossover variation of a two-dimensional Hofmann-type compound

Zhi-Kun Liu,[a†] Ke Sun,[a†] Jin-Peng Xue,[a] Zi-Shuo Yao,[a*] Jun Tao[a*]

[a]*Key Laboratory of Cluster Science of Ministry of Education, School of Chemistry and Chemical Engineering, Liangxiang Campus, Beijing Institute of Technology, Beijing 102488, People's Republic of China.*

[†]*These authors contributed equally to this work.*

E-mail: taojun@bit.edu.cn; zishuoyao@bit.edu.cn

Table of Contents

1. Materials and methods

All reagents and materials were purchased commercially and were used without further purification.

The C, H and N elemental analyses were performed on a EUROVECTER EA3000 analyzer. Powder X-ray diffraction (PXRD) data were recorded on a Bruker D8 Advance Diffractometer with Cu Kα radiation (λ = 1.54056 Å). IR spectra were recorded in the range of 4000–400 cm^{-1} on a Thermo IS5 spectrometer with KBr pellets. Differential scanning calorimetry (DSC) measurements were conducted in an aluminum closed pan on a PerkinElmer DSC 8000. Thermogravimetric (TG) analyses were performed under a nitrogen atmosphere on a TG-DTA 6200 instrument with a heating rate of 10 °C min^{-1}.

Magnetic measurements

Magnetic susceptibilities were determined on a Quantum Design MPMS XL7 magnetometer with a scan rate of 2 K min^{-1}. A field of 5000 Oe was applied in the measured temperature range. Magnetic data were corrected for the sample holder and diamagnetic contributions.

Single-crystal X-ray crystallography

Single-crystal X-ray diffraction (SCXRD) data were collected using a Rigaku Oxford XtaLAB PRO diffractometer with graphite-monochromated Mo Kα radiation (λ = 0.71073 Å). The structure was solved by direct methods and further refined by full-matrix least-squares techniques on F^2 with SHELXL.[1] Non-hydrogen atoms were refined anisotropically, and the hydrogen atoms were generated geometrically and refined isotropically. The ligand locates in special positions of mirror symmetry, we have used Olex2[2] to refine the disordered ligands. For **1·H_2O**, in these heavy-atom structures as it was not possible to see clear electron-density peaks in difference maps which would correspond with acceptable locations for the H atoms bonded to water oxygen O5, the refinements were completed with no allowance for these water H atoms in the models.

CCDC 2257410–2257415 contain the supplementary crystallographic data for this paper. These data can be obtained free of charge via www.ccdc.cam.ac.uk/data_request/cif, or by emailing

data_request@ccdc.cam.ac.uk, or by contacting The Cambridge Crystallographic Data Centre, 12 Union Road, Cambridge CB2 1EZ, UK; fax: +44 1223 336033.

2. Synthesis

Preparation of 4-(o-nitrobenzyl)imino-1,2,4-triazole) (*o*-NTrz)

The ligands were synthesized according to the reported literature procedures.[3]

Preparation of $[Fe^{II}(o\text{-NTrz})_2Pt^{II}(CN)_4]\cdot H_2O$ ($\mathbf{1\cdot H_2O}$)

An aqueous solution (5.0 mL) of $FeSO_4\cdot 7H_2O$ (14.0 mg, 0.05 mmol) and ascorbic acid (5.0 mg) was placed at the bottom of the test tube (inner diameter 1.2 cm, length 14.4 cm) and a mixture of methanol and water (v/v = 2:1, 4 mL) was added as a buffer solvent followed by freshly prepared methanol solution (5.0 mL) *o*-NTrz (21.7 mg, 0.1 mmol) and $K_2[Pt(CN)_4]\cdot 3H_2O$ (5.0 mg, 0.01 mmol) into layers. The tubes were sealed and left to stand in an undisturbed environment and brown flaky crystals were collected after 3 weeks. Yield: ~30% based on $K_2[Pt(CN)_4]$. Elemental analyses (%) calcd for $C_{22}H_{16}FeN_{14}O_5Pt$ ($\mathbf{1\cdot H_2O}$): C, 32.73; H, 2.00; N, 24.29. Found: C, 32.69; H, 2.00; N, 23.63. IR (KBr pellet, cm^{-1}): 3627 (w), 3141 (w), 3092 (w), 2359 (w), 2173 (s), 1523 (s), 1352 (m), 1215 (w), 1166 (w), 1050 (s), 952 (w), 846 (w), 664 (m), 609 (m), 423 (w).

Preparation of $[Fe^{II}(o\text{-NTrz})_2Pt^{II}(CN)_4]$ (1)

The brown flake crystals $\mathbf{1\cdot H_2O}$ were heated under vacuum at 373 K for more than 12 h to obtain dehydrated samples **1**. Elemental analyses (%) calcd for $C_{22}H_{14}FeN_{14}O_4Pt$ (**1**): C, 33.48; H, 1.79; N, 24.84. Found: C, 33.51; H, 1.82; N, 24.89. IR (KBr pellet, cm^{-1}): 3626 (w), 3145 (w), 3087 (w), 2357 (m), 2174 (m), 1523 (m), 1356 (m), 1211 (w), 1161 (w), 1053 (m), 954 (w), 855 (w), 672 (w), 609 (w), 456 (w).

3. Additional Tables

Table S1. Crystal structure and refinement details for compound **1·H_2O** at 280, 240, 150 K.

	1·H_2O		
T / K	280	240	150
Empirical formula	$C_{22}H_{16}FeN_{14}O_5Pt$	$C_{22}H_{16}FeN_{14}O_5Pt$	$C_{22}H_{16}FeN_{14}O_5Pt$
Molecular weight	807.43	807.43	807.43
Crystal system	monoclinic	monoclinic	monoclinic
Space group	*C*2/*m*	*C*2/*m*	*C*2/*m*
a/Å	26.6222(8)	26.2662(9)	26.1950(7)
b/Å	7.2969(2)	7.1043(3)	6.9648(2)
c/Å	15.1034(4)	14.8621(5)	14.6878(4)
α/°	90	90	90
β/°	100.271(3)	100.454(3)	100.680(2)
γ/°	90	90	90
Volume/Å^3	2886.96(14)	2727.28(18)	2633.27(13)
Z	4	4	4
ρ_{calc}g/cm^3	1.858	1.966	2.037
μ/mm^{-1}	5.402	5.719	5.923
F(000)	1560.0	1560.0	1560.0
Goodness-of-fit on F^2	1.059	1.087	1.066
Final R indexes [I>=2σ (I)]	R_1 = 0.0240, wR_2 = 0.0612	R_1 = 0.0302, wR_2 = 0.0701	R_1 = 0.0432, wR_2 = 0.1112
Final R indexes [all data]	R_1 = 0.0309, wR_2 = 0.0642	R_1 = 0.0364, wR_2 = 0.07256	R_1 = 0.0524, wR_2 = 0.1170
CCDC no.	2257412	2257411	2257410

$R_1 = \Sigma| |Fo|-|Fc| |/ \Sigma|Fo|$, $wR_2 = [\Sigma w(Fo^2-Fc^2)^2]/ \Sigma w(Fo^2)^2]^{1/2}$

Table S2. Crystal structure and refinement details for compound **1** at 293, 250, 180 K.

	1		
T / K	293	250	180
Empirical formula	$C_{22}H_{14}FeN_{14}O_4Pt$	$C_{22}H_{14}FeN_{14}O_4Pt$	$C_{22}H_{14}FeN_{14}O_4Pt$
Molecular weight	789.41	789.41	789.41
Crystal system	monoclinic	monoclinic	monoclinic
Space group	$C2/m$	$C2/m$	$C2/m$
a/Å	26.4601(9)	26.2968(16)	26.0552(11)
b/Å	7.2922(3)	7.2061(4)	7.0129(2)
c/Å	15.0392(6)	14.9288(9)	14.6062(5)
α/°	90	90	90
β/°	98.267(4)	98.444(6)	99.248(4)
γ/°	90	90	90
Volume/Å^3	2871.69(19)	2798.3(3)	2634.19(16)
Z	4	4	4
ρ_{calc}g/cm^3	1.826	1.874	1.991
μ/mm^{-1}	5.426	5.569	5.915
F(000)	1520.0	1520.0	1520.0
Goodness-of-fit on F^2	0.968	1.076	1.062
Final R indexes [I>=2σ (I)]	R_1 = 0.0316, wR_2 = 0.0813	R_1 = 0.0352, wR_2 = 0.0916	R_1 = 0.0358, wR_2 = 0.0920
Final R indexes [all data]	R_1 = 0.0441, wR_2 = 0.0922	R_1 = 0.0446, wR_2 = 0.0989	R_1 = 0.0452, wR_2 = 0.1017
CCDC no.	2257415	2257414	2257413

$R_1 = \Sigma| |Fo|-|Fc| |/ \Sigma|Fo|$, $wR_2 = [\Sigma w(Fo^2-Fc^2)^2]/ \Sigma w(Fo^2)^2]^{1/2}$

Table S3. The Fe–N bond lengths in compounds **1·H_2O** and **1** at different temperatures.

	1·H_2O			**1**		
T / K	280	240	150	293	250	180
Fe1–N1 (Å)	2.134(3)	1.934(3)	1.929(5)	2.131(5)	2.027(5)	1.930(5)
Fe1–N2 (Å)	2.182(3)	1.971(4)	1.964(6)	2.189(6)	2.076(8)	1.957(7)
Fe2–N7 (Å)	2.127(3)	2.112(3)	1.927(5)	2.129(5)	2.110(5)	1.928(5)
Fe2–N8 (Å)	2.221(4)	2.197(5)	1.987(6)	2.209(6)	2.172(8)	1.980(7)
Fe1–N_{ave} (Å)	2.158(3)	1.953(4)	1.947(6)	2.160(6)	2.052(1)	1.944(1)
Fe2–N_{ave} (Å)	2.174(4)	2.155(4)	1.957(6)	2.169(5)	2.141(6)	1.954(6)
Fe1–N≡C (°)	177.1(3)	178.7(3)	176.7(54)	172.1(3)	174.2(6)	176.6(9)
Fe2–N≡C (°)	170.1(3)	170.0(3)	172.1(4)	169.5(6)	169.6(0)	173.0(8)

Table S4. The π···π, hydrogen-bonding interaction distances and Fe···Fe distances for **1·H_2O** and **1.**

	1·H_2O			**1**		
T / K	280	240	150	293	250	180
π···π interations (Å)	3.783(1)/ 3.927(1)	3.760(1)/ 3.818(1)	3.676(1)/ 3.861(1)	3.774(9)/ 3.899(0)	3.785(4)/ 3.840(0)	3.703(9)/ 3.813(4)
O5–N3 (Å)	2.910(6)	2.842(8)	2.78 5(9)			
d1 (Å)	7.297(2)	7.104(3)	6.965(2)	7.292(2)	7.206(1)	7.012(9)
d2 (Å)	7.552(2)	7.431(3)	7.344(2)	7.519(6)	7.464(4)	7.303(1)

4. Additional Figures

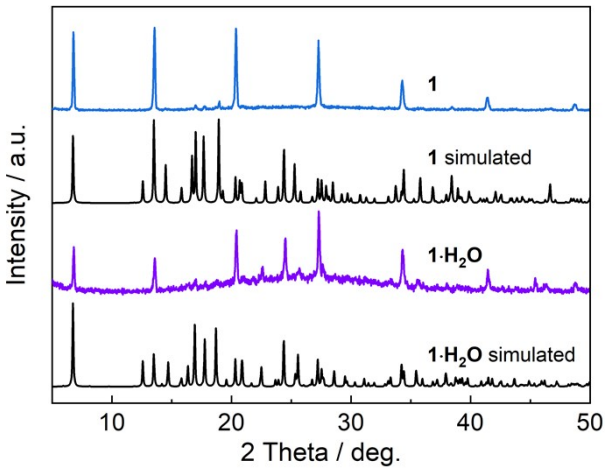

Fig. S1 PXRD patterns of compounds **1·H_2O** and **1**.

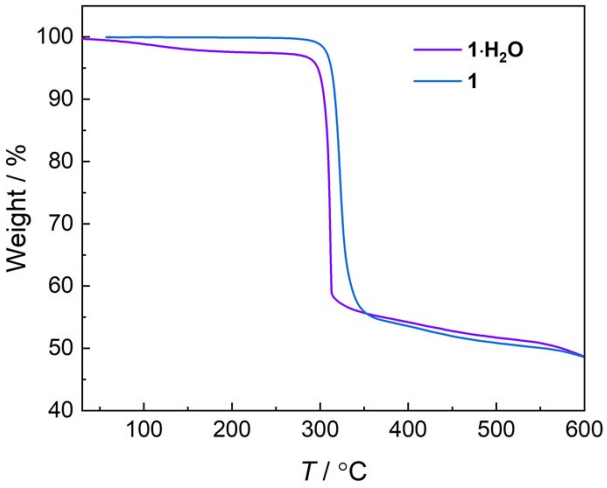

Fig. S2 TGA curves of **1·H_2O** and **1**. The variation of guest water molecules was supported by the TGA measurements. The mass loss of around 2.42 % for **1·H_2O** is proximal to the calculated value of 2.24 % for a single water molecule. In contrast, no significant weight reduction was observed in the crystal of **1**.

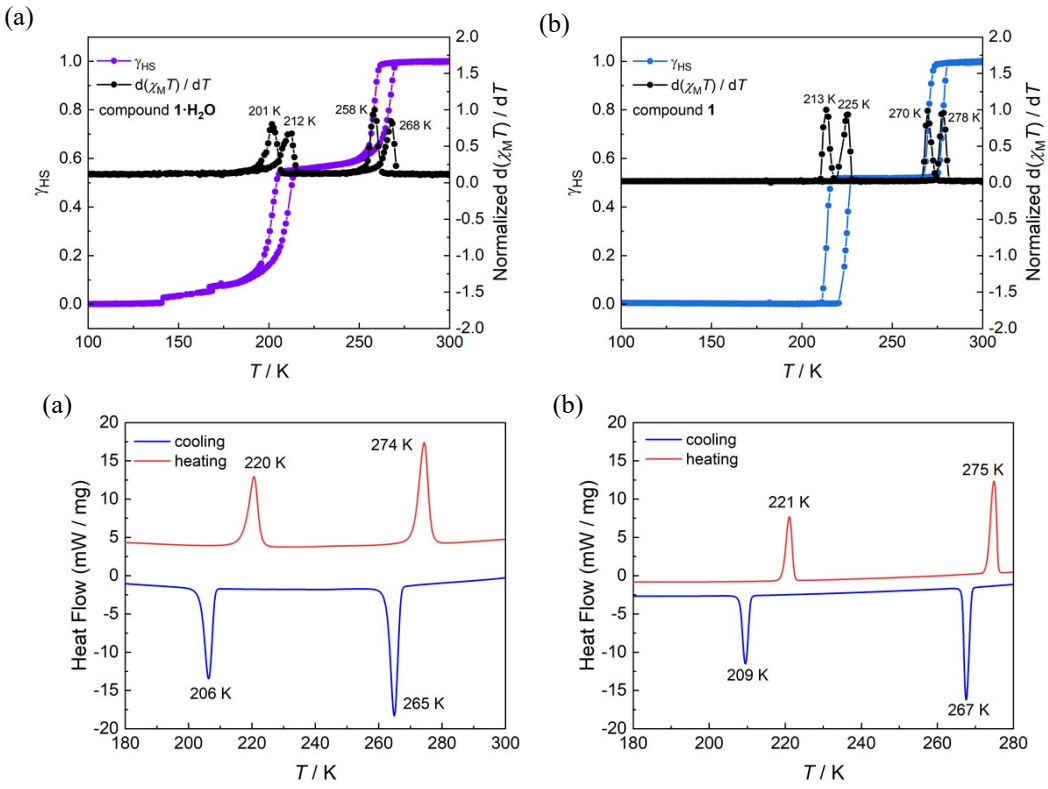

Fig. S3 HS fraction (γ_{HS}) and normalized $\partial(\chi_M T)$ versus T plots of **1·H$_2$O** (a) and **1** (b).

Fig. S4 DSC curves of **1·H$_2$O** (a) and **1** (b) upon cooling and warming.

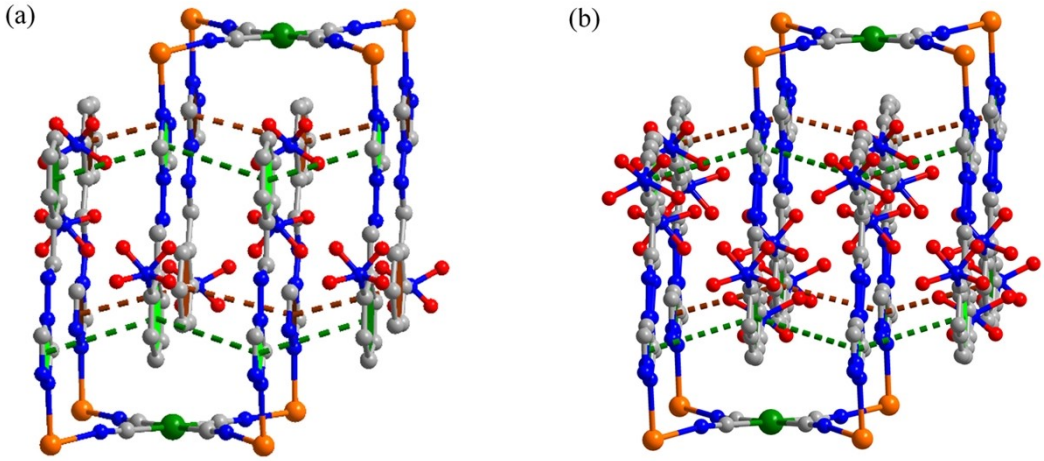

Fig. S5 Adjacent layers showing interlayer ligand π···π interactions for **1·H$_2$O** (a) and **1** (b). The interlayer π···π interactions in SCO compounds stabilize the structure, allowing the large rearrangement of the structure in response to the dehydration of the crystals.

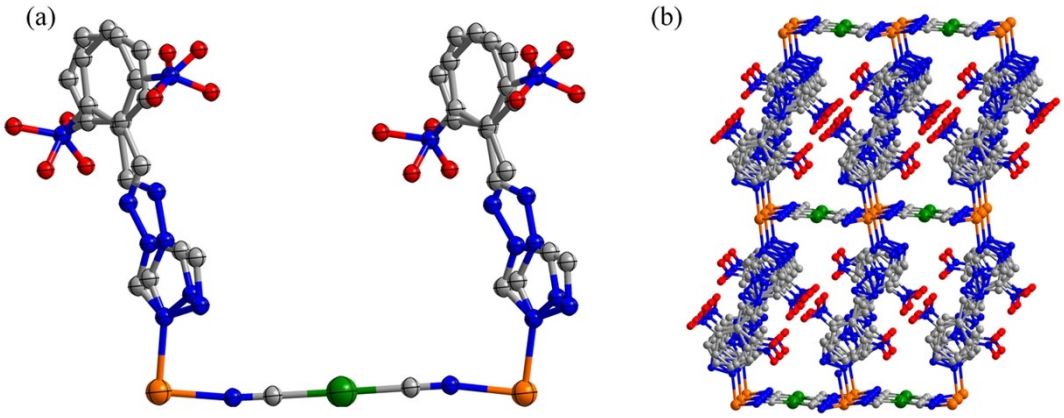

Fig. S6 (a) The asymmetric unit of compound **1** at 293 K. (b) 3D Stacked Layers. Hydrogen atoms are omitted for clarity.

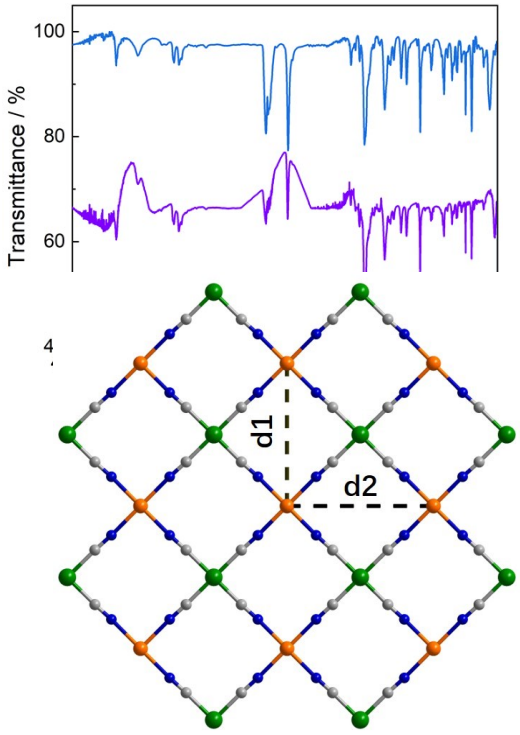

Fig. S7 FT-IR spectra of **1·H$_2$O** and **1**.

Fig. S8 The Fe···Fe distances in the 2D $[FePt(CN)_4]_n$ layer.

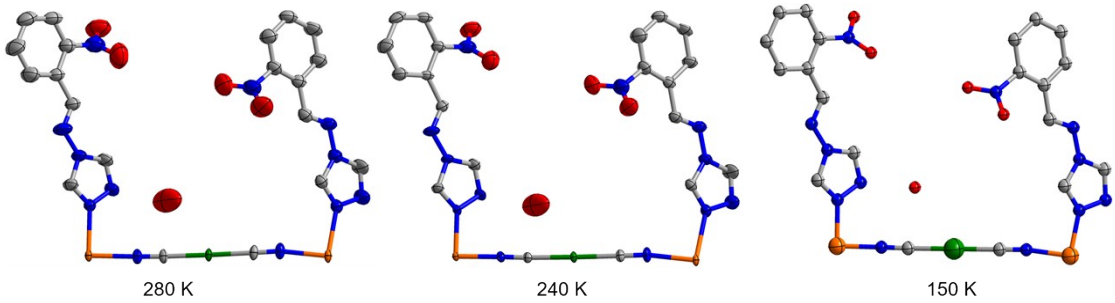

Fig. S9 The asymmetric unit of compound **1·H_2O**, showing thermal ellipsoids at 50% probability level. (Hydrogen atoms are omitted for clarity, baby blue is the disordered; C: dark grey; N: blue; Fe: orange; O: red; Pt: green.)

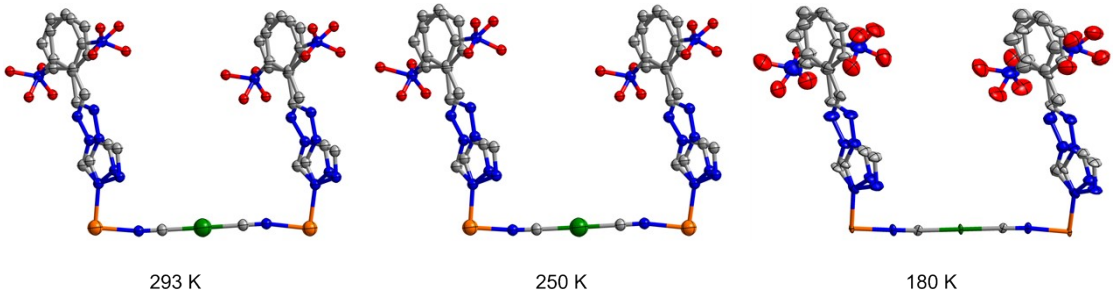

Fig. S10 The asymmetric unit of compound **1**, showing thermal ellipsoids at 50% probability level. (Hydrogen atoms are omitted for clarity, baby blue is the disordered; C: dark grey; N: blue; Fe: orange; O: red; Pt: green.)

5 References

1 J. E. Clements, P. R. Airey, F. Ragon, V. Shang, C. J. Kepert and S. M. Neville, *Inorg. Chem.*, 2018, **57**, 14930–14938.

2 G. M. Sheldrick, *Acta Cryst. C*, 2015, **71**, 3–8.

3 O. V. Dolomanov, L. J. Bourhis, R. J. Gildea, J. A. K. Howard and H. Puschmann, *J. Appl. Crystallogr.*, 2009, **42**, 339–341.